

**THE SYSTEM  $\text{MgO-SiO}_2\text{-H}_2\text{O}$  AT  
HIGH PRESSURES AND TEMPERATURES —  
STABILITY FIELD FOR HYDROXYL-CHONDRODITE,  
HYDROXYL-CLINOHUMITE AND 10 Å-PHASE**

KATSUHIRO YAMAMOTO\* and SYUN-ITI AKIMOTO\*\*

**ABSTRACT.** The system  $\text{MgO-SiO}_2\text{-H}_2\text{O}$  was investigated at pressures between 29 and 77 kb and at temperatures between 470° and 1225°C. Reaction products were examined by X-ray, optical, and thermal analysis. Brucite, phase A, phase D, clinohumite, forsterite, serpentine, orthoenstatite, clinoenstatite, talc, 10 Å-phase, quartz, and coesite were synthesized. Hydroxyl-clinohumite was first obtained in the present experiments. The chemical formula of phase D was determined as  $\text{H}_2\text{Mg}_5\text{Si}_5\text{O}_{10}$ ,  $[\text{Mg}(\text{OH})_2 \cdot 2\text{Mg}_2\text{SiO}_4]$ , and the phase was established to be hydroxyl-chondrodite. Although both chondrodite and clinohumite are stable only in rocks much richer in MgO than the accepted mantle rocks, they are of considerable interest as possible sites for  $\text{H}_2\text{O}$  in the upper mantle.

INTRODUCTION

Experimental information on the stability, phase relationships, and physical properties in the system  $\text{MgO-SiO}_2\text{-H}_2\text{O}$  throws light upon the hydration and dehydration process in the crust and mantle, the metamorphism in the crust, and the effect of water vapor on the melting of magnesium silicates.

Systematic investigation of the system  $\text{MgO-SiO}_2\text{-H}_2\text{O}$  was initiated by Bowen and Tuttle (1949). They determined the stability fields of brucite  $\text{Mg}(\text{OH})_2$ , forsterite  $\text{Mg}_2\text{SiO}_4$ , serpentine  $\text{Mg}_3[\text{Si}_2\text{O}_5](\text{OH})_4$ , enstatite  $\text{MgSiO}_3$ , talc  $\text{Mg}_3[\text{Si}_4\text{O}_{10}](\text{OH})_2$ , and quartz at pressures to approx 3 kb and temperatures to 1000°C. Kitahara, Takenouchi, and Kennedy (1966) extended the pressure range up to 30 kb. Sclar, Carrison, and Schwartz (1965) and Sclar and Carrison (1966) reported the synthesis of the 10 Å-phase in the system  $\text{MgO-SiO}_2\text{-H}_2\text{O}$  at pressures between 32 and 90 kb and at temperatures between 375° and 525°C. Ringwood and Major (1967) investigated this system at pressures between 100 and 180 kb and at temperatures between 600° and 1100°C and discovered three new phases denoted A, B, and C. Yamamoto and Akimoto (1974) investigated this system at pressures between 40 and 95 kb and at temperatures between 500° and 1400°C. They determined the stability field and the chemical formula of phase A,  $\text{H}_6\text{Mg}_7\text{Si}_2\text{O}_{14}$ , and found a new phase denoted D.

The present experiments were carried out to determine the chemical formula of phase D and to examine the phase relationships of the system  $\text{MgO-SiO}_2\text{-H}_2\text{O}$  at pressures between 29 and 77 kb and at temperatures between 500° and 1200°C.

EXPERIMENTAL PROCEDURE

Mixtures of guaranteed grades of the reagents  $\text{Mg}(\text{OH})_2$  and silicic acid ( $\text{SiO}_2 \cdot y\text{H}_2\text{O}$ ) were used as starting materials. In some runs for 10

\* Water Research Institute, Nagoya University, Chikusa-ku, Nagoya 464, Japan

\*\* Institute for Solid State Physics, The University of Tokyo, Roppongi, Minato-ku, Tokyo 106, Japan

$\bar{A}$ -phase, a certain amount of distilled water was added to the mixtures.  $\text{Mg}(\text{OH})_2$  was used instead of  $\text{MgO} + \text{H}_2\text{O}$  because of ease of treatment. Water content of the silicic acid was determined to be 4.74 wt percent ( $y = 0.166$ ) by the ignition loss after heat treatment at  $900^\circ\text{C}$  for 6 hrs. The compositions of mixtures,  $x'\text{Mg}(\text{OH})_2 + \text{SiO}_2 \cdot y\text{H}_2\text{O} = (x' + y)\text{H}_2\text{O} + x'\text{MgO} + \text{SiO}_2$ , were determined from mixing ratios of  $\text{Mg}(\text{OH})_2$  to  $\text{SiO}_2 \cdot y\text{H}_2\text{O}$ . The mixtures of  $x' = 3/8, 1/2, 5/8, 3/4, 7/8, 1, 3/2, 7/4, 2, 17/8, 9/4, 7/3, 5/2, 11/4, 3, 7/2, 4,$  and  $5$  were prepared. These were labeled by  $x = 100x'/(1+x')$  percent which was  $\text{MgO}$  mol percent calculated for anhydrous composition. The relation of  $x$  to  $x'$  is shown in figure 1, where the compositions of starting materials are represented on a triangular diagram, the system  $\text{MgO}-\text{SiO}_2-\text{H}_2\text{O}$ .

A tetrahedral-anvil type of high-pressure apparatus was used. Anvils with 20 mm edge and pyrophyllite tetrahedrons with 25 mm edge were used from 29 to 60 kb, and anvils with 15 mm edge and pyrophyllite tetrahedrons with 20 mm edge were also used in the range 29 to 77 kb. The pressure values were calibrated at room temperature on the basis

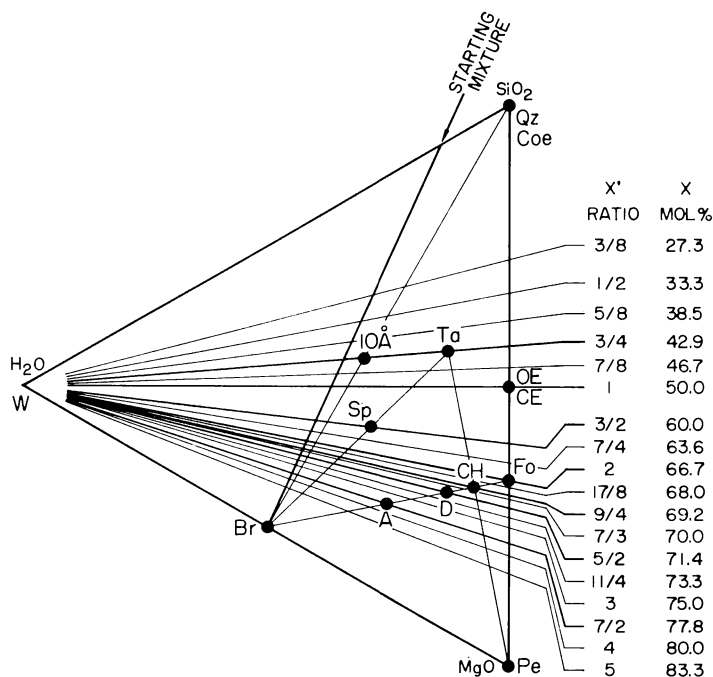


Fig. 1. The system  $\text{MgO}-\text{SiO}_2-\text{H}_2\text{O}$ . Compositions of all the starting mixtures are represented by cross points between a line labeled with "starting mixture" and lines with constant  $\text{MgO}/\text{SiO}_2$  mol ratio. The compositions of phases that occurred in the present experiments are plotted by solid circles. Abbreviations: Pe, periclase; Br, brucite; A, phase A; D, phase D (chondrodite); CH, clinohumite; Fo, forsterite; Sp, serpentine; OE, orthoenstatite; CE, clinoenstatite; Ta, talc; 10  $\bar{A}$ , 10  $\bar{A}$ -phase; Qz, quartz; Coe, coesite; W, water.

of the pressure scale recommended at the U.S. National Bureau of Standards Symposium, 1968, using resistance transitions of Bi I-II (25.5 kb), Ba I-II (55 kb), and Bi III-V (77 kb). Since the reproducibility of the pressure calibration is good, the precision of the relative pressure determinations was estimated to be  $\pm 2$  percent.

The desired temperature was obtained using cylindrical graphite heaters placed in the central part of the pyrophyllite tetrahedrons. To prevent water loss during the run, starting materials were placed in Au tubes of 1.2 mm outer diameter (OD) and 1.0 mm inner diameter (ID) or 1.6 mm OD and 1.4 mm ID and sealed by dc carbon arc welding. Details of the furnace assembly were described in a previous paper (Yamamoto and Akimoto, 1974). Temperature was measured by a Pt/Pt-13 percent Rh thermocouple in contact with the Au tubes. No correction was made for the effect of pressure on the emf of the thermocouple. The precision of the temperature measurements is estimated to be  $\pm 20^\circ\text{C}$  at  $600^\circ\text{C}$  and  $\pm 30^\circ\text{C}$  at  $1000^\circ\text{C}$  based on a previous measurement of the temperature gradient within the graphite furnace using the tetrahedral-anvil press (Akimoto, Fujisawa, and Katsura, 1965).

As many as three capsules could be loaded into a heater and then run simultaneously at a given temperature and pressure. The synthesis of phase D to obtain material for thermal analysis was carried out in Au foil of  $30\ \mu\text{m}$  thickness instead of a tube in order to obtain as much material as possible. In this case temperature was estimated from the electric power of the heating element.

Runs varied from 0.5 to 12 hrs depending upon the reaction temperature. Run times were generally longer than or equal to those used by Kitahara, Takenouchi, and Kennedy (1966) in the experiments of the system  $\text{MgO-SiO}_2\text{-H}_2\text{O}$  using oxide starting mixtures. Since Kitahara, Takenouchi, and Kennedy showed that the phase boundaries determined from such an experimental procedure were always in close agreement with those determined from the reverse reactions with longer intervals of run time, we considered that the phase boundaries determined in the present investigation approx represent equilibrium boundaries, although no reverse reactions were carried out. Pressure and temperature fluctuations during the runs were controlled to  $\pm 2$  kb and to  $\pm 20^\circ\text{C}$ .

Samples were quenched isobarically and examined by powder X-ray diffraction technique after each run. Structure determination of the samples was carried out with the aid of a Weissenberg camera when single crystals were available.  $\text{Cu K}\alpha$  radiation was used throughout the X-ray analyses. In order to determine the degree of hydration of phase D, the samples of this phase synthesized at 50 kb and approx  $900^\circ\text{C}$  were examined using a thermobalance, Rigaku Denki thermoflex 8002 type, in a self-generating atmosphere under a heating rate of  $5^\circ\text{C}/\text{min}$ .  $\alpha\text{-Al}_2\text{O}_3$  of the same mass as the samples was used as a reference material for differential thermal analyses. At each reaction observed in the thermograph, the structure of the samples was examined using X-ray diffraction. The

refractive indices of clinohumite synthesized from the mixture of  $x = 71.4$  percent at 77 kb and 1130°C were measured by the Becke-line method and compared with that of natural clinohumite given in the reference by Deer, Howie, and Zussman (1971).

#### EXPERIMENTAL RESULTS

Reaction products of the present experiments are brucite, phase A, phase D, clinohumite, forsterite, serpentine, orthoenstatite, clinoenstatite, talc, 10 Å-phase, quartz, and coesite. These were distinguished using a X-ray diffractometer and a Weissenberg camera. Effusion of water from the tube when it was cut or a significant degree of wetness of the sample were taken as indications that H<sub>2</sub>O had been produced by the reaction. Pressure and temperature conditions and results of runs are listed in table 1. Chemical compositions of these reaction products are given in table 2 and plotted on the MgO-SiO<sub>2</sub>-H<sub>2</sub>O triangular diagram (fig. 1).

The 10 Å-phase was identified in mixtures of  $x \leq 71.4$  percent above 40 kb and below 725°C. Talc was identified in mixtures of  $x \leq 60.0$  percent below 48 kb and 830°C. Orthoenstatite was identified from mixtures of  $x \leq 60.0$  percent above 625°C. Clinoenstatite was identified in mixtures of  $x \leq 75.0$  percent above 60 kb and between 535° and 930°C. Serpentine was identified in mixtures of 50.0 percent  $\leq x \leq 70.0$  percent below 48 kb and below 615°C. Forsterite was identified in mixtures of  $x \geq 50.0$  percent. Clinohumite was identified in mixtures of 68.0 percent  $\leq x \leq 75.0$  percent above 730°C. Phase D was identified in mixtures of  $x \geq 70.0$  percent above 730°C. Phase A was identified in mixtures of  $x \geq 60.0$  percent above 55 kb and below 935°C.

Figure 2A, B, C, D, E, F, and G are isobaric synthesis diagrams that represent the products of these experiments at 29, 40, 48, 55, 60, 72, and 77 kb. In figure 2, open circles indicate experimental runs in which the observed assemblage directly corresponds to the labeled phase area of the diagram; solid circles indicate runs in which the observed assemblage appears to be a mixture of the assemblages that appear above and below a given temperature boundary line.

The synthesis diagrams of figure 2 are consistent with a pressure-temperature equilibrium phase diagram shown in figure 3A, B, and C, which contains eleven invariant points and their associated lines of univariant equilibrium and areas of divariant equilibrium. Figures 3A and B stand for the pressure-temperature diagram for the compositional range,  $\text{MgO/SiO}_2 \leq 2$  and  $\text{MgO/SiO}_2 \geq 2$ , respectively. Composition-paragenesis diagrams around eight significant invariant points are shown in figure 3C.

Talc coexists with water up to approx 55 kb, and the 10 Å-phase is stable up to approx 725°C. The 10 Å-phase is formed by the hydrations of talc, enstatite, serpentine, forsterite, and phase A and is stable for any composition on the join  $\text{Mg(OH)}_2\text{-SiO}_2$  in the region of 55 kb and 475°C. The field in which enstatite coexists with water expands to low temperature regions with increasing pressure. Serpentine coexists with

TABLE I  
Conditions and results of runs

Run No.	P <sup>†</sup> (kbar)	T <sup>††</sup> (°C)	Run Time (hours)	Starting Materials (x%)	Results	Run No.	P (kbar)	T (°C)	Run Time (hours)	Starting Materials (x%)	Results
7376	29	580	4	33.3	Ta + Qz + W	7329	48	775	3	42.9	OE + Coe + W
7328	29	830	3	42.9	OE + Ta + Qz + W*	7359	48	725	2	46.7	OE + Ta + W
7304	29	495	12	50.0	Sp + Ta + W	7305	48	495	12	50.0	Fo + Sp + 10Å(I) + W*
7309	29	615	5	50.0	Fo + Sp + Ta + W*	7312	48	545	8	50.0	Fo + 10Å(I) + W
7302	29	715	4	50.0	Fo + Ta + W	7315	48	615	5	50.0	Fo + 10Å(I) + W
7310	29	770	3	50.0	Fo + OE + Ta + W*	7317	48	660	5	50.0	Fo + Ta + W
7367	29	1125	0.5	50.0	OE + W	7314	48	730	4	50.0	OE + W
7304	29	495	12	60.0	Sp + W	7305	48	495	12	60.0	Fo + Sp + 10Å(I) + W*
7306	29	540	8	60.0	Sp + W	7312	48	545	8	60.0	Fo + 10Å(I) + W
7376	29	580	4	60.0	Sp + W	7315	48	615	5	60.0	Fo + 10Å(I) + W
7309	29	615	5	60.0	Fo + Sp + Ta + W*	7314	48	730	4	60.0	Fo + OE + W
7302	29	715	4	60.0	Fo + Ta + W	7313	48	825	2	60.0	Fo + OE + W
7310	29	770	3	60.0	Fo + OE + Ta + W*	7305	48	495	12	66.7	Fo + W
7307	29	815	3	60.0	Fo + OE + W	7317	48	660	5	69.2	Br + Fo + W
7376	29	580	4	63.6	Fo + Sp + W	7370	48	1025	1	69.2	Br + CH + Fo + W**
7306	29	540	8	66.7	Fo + W	7366	48	1135	0.5	69.2	Br + Fo + W**
7367	29	1125	0.5	66.7	Fo + W	7312	48	545	8	70.0	Br + Fo + W
7304	29	495	12	68.0	Br + Sp + W	7314	48	730	4	70.0	Br + D + CH + Fo + W*
7302	29	715	4	68.0	Br + Fo + W	7313	48	825	2	70.0	D + CH + W
7303	29	925	2	68.0	CH + Fo + W	7317	48	660	5	71.4	Br + Fo + W
7306	29	540	8	69.2	Br + Fo + W	7370	48	1025	1	71.4	Br + D + CH + W**
7328	29	830	3	69.2	CH + W	7366	48	1135	0.5	71.4	Br + Fo + W**
7369	29	965	1	69.2	Br + CH + Fo + W**	7313	48	825	2	75.0	Br + D + W
7364	29	1125	0.5	69.2	Br + Fo + W**	7370	48	1025	1	75.0	Br + D + W**
7301	29	735	4	70.0	Br + Fo + W	7366	48	1135	0.5	75.0	Br + Fo + W**
7307	29	815	3	70.0	Br + D + CH + Fo + W*						
7303	29	925	2	70.0	D + CH + W	7210	50	840	3	71.4	D + W
7301	29	735	4	71.4	Br + Fo + W	7211	50	1040	2	71.4	Br + D + CH + W**
7369	29	965	1	71.4	Br + D + CH + W**	7219	50	1110	2	71.4	Br + CH + Fo + W**
7209	29	1030	2.5	71.4	Br + D + CH + W**	7218	50	1220	1	71.4	Br + Fo + W**
7364	29	1125	0.5	71.4	Br + Fo + W**						
7301	29	735	4	73.3	Br + Fo + W	7374	55	570	6	33.3 + W	10Å(II) + Coe + W

7307	29	815	3	75.0	Br + D + Fo + W*	7371	55	570	9.5	38.5	$10\overset{\circ}{A}(II) + Coe$
7303	29	925	2	75.0	Br + D + W	7371	55	570	9.5	38.5 + W	$10\overset{\circ}{A}(I) + Coe$
7369	29	965	1	75.0	Br + D + W**	7373	55	570	5	38.5 + W	$10\overset{\circ}{A}(I) + 10\overset{\circ}{A}(II) + Coe + w$
7364	29	1125	0.5	75.0	Br + Fo + W**	7375	55	570	5	38.5 + W	$10\overset{\circ}{A}(II) + Coe + w$
7367	29	1125	0.5	77.8	Br + Fo + W**	7377	55	570	6	38.5 + W	$10\overset{\circ}{A}(II) + Coe + W$
						7324	55	625	6	38.5 + W	$10\overset{\circ}{A}(I) + 10\overset{\circ}{A}(II) + Coe + w$
7034	38	505	4.5	66.7	Br + Sp + W	7365	55	570	9.5	42.9	$10\overset{\circ}{A}(II)$
7036	38	550	4.5	66.7	Fo + W	7365	55	570	9.5	42.9 + W	$10\overset{\circ}{A}(I)$
						7379	55	570	7	42.9 + W	$10\overset{\circ}{A}(I) + w$
7363	40	735	2	38.5	Ta + Coe + W	7324	55	625	6	42.9 + W	$10\overset{\circ}{A}(I) + w$
7360	40	785	2	38.5	OE + Ta + Coe + W*	7323	55	680	4	46.7	$OE + 10\overset{\circ}{A}(I) + W$
7363	40	735	2	42.9	Ta + W	7358	55	470	10	50.0	$Br + 10\overset{\circ}{A}(I) + w$
7330	40	765	3	42.9	Ta + W	7324	55	625	6	50.0 + W	$Fo + OE + 10\overset{\circ}{A}(I) + W^*$
7360	40	785	2	42.9	OE + Ta + Coe + W*	7358	55	470	10	60.0	$Br + 10\overset{\circ}{A}(I) + w$
7363	40	735	2	46.7	OE + Ta + W	7358	55	470	10	71.4	$Br + 10\overset{\circ}{A}(I) + w$
7360	40	785	2	46.7	OE + Ta + Coe + W*	7357	55	760	2	75.0	$Br + A + D + W^*$
7308	40	495	12	50.0	Sp + $10\overset{\circ}{A}(I) + w$	7357	55	760	2	77.8	$Br + A + D + W^*$
7319	40	560	6	50.0	Fo + Sp + Ta + $10\overset{\circ}{A}(I) + W^*$	7323	55	680	4	80.0	$Br + A + W$
7318	40	620	5	50.0	Fo + Ta + W	7357	55	760	2	80.0	$Br + A + D + W^*$
7320	40	675	5	50.0	Fo + Ta + W						
7308	40	495	12	60.0	Sp + W	7348	60	475	10	33.3	$10\overset{\circ}{A}(I) + 10\overset{\circ}{A}(II) + Coe + w$
7319	40	560	6	60.0	Fo + Sp + Ta + $10\overset{\circ}{A}(I) + W^*$	7327	60	695	3.5	42.9	$10\overset{\circ}{A}(II)$
7318	40	620	5	60.0	Fo + Ta + W	7355	60	725	2	42.9	$OE + 10\overset{\circ}{A}(I) + 10\overset{\circ}{A}(II) + Coe + W^*$
7320	40	675	5	60.0	Fo + Ta + W	7326	60	775	3	42.9	$OE + Coe + W$
7316	40	745	4	60.0	Fo + OE + W	7351	60	630	3	46.7	$CE + 10\overset{\circ}{A}(I) + W$
7308	40	495	12	70.0	Br + Fo + Sp + W*	7322	60	580	7.5	50.0	$Fo + 10\overset{\circ}{A}(I) + W$
7319	40	560	6	70.0	Br + Fo + W	7325	60	675	4.5	50.0	$CE + W$
7318	40	620	5	70.0	Br + Fo + W	7321	60	735	4	50.0	$OE + W$
7316	40	745	4	70.0	Br + D + CH + Fo + W*	7348	60	475	10	60.0	$A + 10\overset{\circ}{A}(I) + W$
7316	40	745	4	75.0	Br + D + Fo + W*	7354	60	515	5	60.0	$A + 10\overset{\circ}{A}(I) + W$
						7356	60	820	1.5	60.0	$Fo + OE + W$
7359	48	725	2	42.9	Ta + W	7022	60	580	3.5	66.7	$A + 10\overset{\circ}{A}(I) + W$
						7021	60	630	2	66.7	$Fo + W$

TABLE I (continued)

Run No.	P (kbar)	T (°C)	Run Time (hours)	Starting Materials (x%)	Results	Run No.	P (kbar)	T (°C)	Run Time (hours)	Starting Materials (x%)	Results
7336	72	475	10	83.3	Br + A + W	7322	60	580	7.5	69.2	A + Fo + W
7350	72	1220	0.5	83.3	Br + D + W**	7326	60	775	3	69.2	CH + W
7381	77	650	3	38.5 + W	10Å(I) + Coe + W	7352	60	875	1.5	69.2	CH + W
7381	77	650	3	42.9	10Å(II)	7354	60	515	5	71.4	A + 10Å(I) + W
7062	77	735	2	50.0	CE + W	7351	60	630	3	71.4	A + Fo + W
7064	77	930	1	50.0	CE + W	7355	60	725	2	71.4	A + Fo + W
7067	77	1125	0.5	50.0	OE + W	7212	60	1050	2	71.4	Br + D + CH + W**
7062	77	735	2	60.0	A + CE + W	7326	60	775	3	75.0	A + D + W
7064	77	930	1	60.0	Fo + CE + W	7356	60	820	1.5	77.8	A + W
7067	77	1125	0.5	60.0	Fo + OE + W	7352	60	875	1.5	77.8	Br + D + W**
7061	77	725	2	66.7	A + CE + W	7348	60	475	10	83.3	Br + A + W
7214	77	1025	2	66.7	Fo + W	7322	60	580	7.5	83.3	Br + A + W
7206	77	835	3	69.2	A + Fo + W	7321	60	735	4	83.3	Br + A + W
7378	77	880	1.5	69.2	CH + W	7028	65	705	3	66.7	Fo + W
7205	77	950	2	69.2	CH + W	7015	70	515	2.5	66.7	A + 10Å(I) + W
7208	77	1025	2	69.2	CH + W	7011	70	695	2	66.7	A + CE + W
7215	77	1150	1.5	69.2	Br + Fo + W**	7014	70	750	2	66.7	A + Fo + CE + W*
7061	77	725	2	71.4	A + CE + W	7020	70	785	2	66.7	Fo + W
7380	77	785	2	71.4	A + CE + W	7213	70	1040	2	71.4	D + W
7202	77	830	3	71.4	A + Fo + W	7336	72	475	10	27.3	10Å(I) + 10Å(II) + Coe + w
7378	77	880	1.5	71.4	A + D + CH + W*	7334	72	925	1	33.3	CE + Coe + W
7201	77	920	2	71.4	D + W	7350	72	1220	0.5	33.3	OE + Coe + W
7065	77	925	1	71.4	D + W	7342	72	575	4	38.5	10Å(II) + Coe
7204	77	1035	2	71.4	Br + D + CH + W**	7338	72	630	3	38.5	10Å(II) + Coe
7203	77	1110	2	71.4	Br + CH + W**	7340	72	725	2	38.5	CE + Coe + W
7068	77	1140	0.5	71.4	Br + CH + Fo + W**	7342	72	575	4	42.9	10Å(II)
7217	77	1220	1	71.4	Br + Fo + W**	7384	72	630	11	42.9 + W	10Å(I) + W
7207	77	1020	2	73.3	Br + D + W**	7346	72	680	3	42.9	CE + 10Å(I) + 10Å(II) + Coe + W*
7216	77	1160	1	73.3	Br + CH + W**	7342	72	575	4	46.7	CE + 10Å(I) + W
7061	77	725	2	75.0	A + CE + W						
7065	77	925	1	75.0	A + D + W						
7068	77	1140	0.5	75.0	Br + D + W**						

7340	72	725	2	46.7	CE + Coe + W
7344	72	535	5	50.0	CE + W
7334	72	925	1	50.0	CE + W
7347	72	1225	0.5	50.0	OE + W
7336	72	475	10	60.0	A + 10Å(I) + W
7334	72	925	1	60.0	Fo + CE + W
7350	72	1220	0.5	60.0	Fo + OE + W
7338	72	630	3	66.7	A + CE + W
7339	72	815	1.5	66.7	Fo + W
7341	72	1025	1	66.7	Fo + W
7347	72	1225	0.5	66.7	Fo + W
7339	72	815	1.5	69.2	A + Fo + W
7345	72	875	1.5	69.2	CH + W
7349	72	975	1	69.2	CH + W
7341	72	1025	1	69.2	Br + CH + Fo + W**
7361	72	1125	0.7	69.2	Br + Fo + W**
7335	72	935	1	70.0	D + CH + W
7340	72	725	2	71.4	A + CE + W
7343	72	770	2	71.4	A + Fo + W
7339	72	815	1.5	71.4	A + Fo + W
7345	72	875	1.5	71.4	A + D + CH + W**
7349	72	975	1	71.4	D + W
7341	72	1025	1	71.4	Br + D + CH + W**
7361	72	1125	0.7	71.4	Br + CH + W**
7353	72	1220	0.5	71.4	Br + Fo + W**
7345	72	875	1.5	75.0	A + D + CH + W*
7335	72	935	1	75.0	Br + A + D + W*,**
7361	72	1125	0.7	75.0	Br + D + W**
7353	72	1220	0.5	75.0	Br + Fo + W**
7338	72	630	3	77.8	A + W
7335	72	935	1	77.8	Br + A + D + W*,**
7349	72	975	1	77.8	Br + D + W**
7353	72	1220	0.5	77.8	Br + Fo + W**

† Precision of pressure measurement and control is about ±2 kbar.

†† Precision of temperature measurement is about ±20°C at 600°C and ±30°C at 1000°C. Temperature fluctuation during runs is less than ±20°C.

\* Four-phase assemblages are considered to be on or close to univariant lines. Interpretation for five-phase assemblages is given in the text

\*\* Brucite + water was formed during quenching from periclase + water and from water in which MgO was dissolved.

Abbreviations : Br; brucite, A; phase A, D; phase D, CH; clinohumite, Fo; forsterite, Sp; serpentine, CE; clinoenstatite, OE; orthoenstatite, Ta; talc, 10Å(I); type I of 10Å-phase, 10Å(II); type II of 10Å-phase, Qz; quartz, Coe; coesite, W; water, w; wetness.

TABLE 2  
Compositions of phases that occur in the system MgO–SiO<sub>2</sub>–H<sub>2</sub>O

Phase	Formula	Mol ratio			Mol fraction		
		MgO	SiO <sub>2</sub>	H <sub>2</sub> O	MgO	SiO <sub>2</sub>	H <sub>2</sub> O
Brucite	Mg(OH) <sub>2</sub>	1	0	1	0.5	0	0.5
Phase A	3Mg(OH) <sub>2</sub> • 2Mg <sub>2</sub> SiO <sub>4</sub>	7	2	3	0.583	0.167	0.25
Phase D (hydroxyl–chondrodite)	Mg(OH) <sub>2</sub> • 2Mg <sub>2</sub> SiO <sub>4</sub>	5	2	1	0.625	0.25	0.125
Hydroxyl–clinohumite	Mg(OH) <sub>2</sub> • 4Mg <sub>2</sub> SiO <sub>4</sub>	9	4	1	0.643	0.286	0.071
Forsterite	Mg <sub>2</sub> SiO <sub>4</sub>	2	1	0	0.667	0.333	0
Serpentine	Mg <sub>3</sub> Si <sub>2</sub> O <sub>5</sub> (OH) <sub>4</sub>	3	2	2	0.428	0.286	0.286
Orthoenstatite	} MgSiO <sub>3</sub>	1	1	0	0.5	0.5	0
Clinoenstatite							
Talc	Mg <sub>3</sub> Si <sub>4</sub> O <sub>10</sub> (OH) <sub>2</sub>	3	4	1	0.375	0.5	0.125
10 Å-phase	Mg <sub>3</sub> Si <sub>4</sub> O <sub>10</sub> (OH) <sub>2</sub> • 2H <sub>2</sub> O	3	4	3	0.3	0.4	0.3
(10 Å-phase, Sclar, Carrison, and Schwartz)	(H <sub>3</sub> O) <sub>2</sub> Mg <sub>3</sub> Si <sub>8</sub> O <sub>20</sub> • 2H <sub>2</sub> O	5	8	5	0.278	0.444	0.278
Quartz	} SiO <sub>2</sub>	0	1	0	0	1.0	0
Coesite							

water up to approx 480°C. Clinohumite is stable above approx 700°C. This phase is formed from brucite + forsterite and phase A + forsterite by solid-solid reaction and from forsterite + magnesium-rich water. The upper stability limit of clinohumite depends upon the bulk composition of the reaction system. Phase D is stable above approx 700°C. This phase is formed from brucite + clinohumite and phase A + clinohumite by solid-solid reaction, from the decomposition of phase A, and from clinohumite + magnesium-rich water. The upper stability limit of phase D depends upon the bulk composition of the reaction system. Phase A is stable above approx 50 kb.

Brucite in the sample reacted in the stability region of periclase + water and at temperatures below about 1000°C may be formed during quenching as suggested by Yamaoka, Fukunaga, and Saito (1970). The equilibrium curve between brucite and periclase + water determined by Yamaoka, Fukunaga, and Saito is extrapolated to higher pressures and is shown in figures 2 and 3.

There is a possibility that the 10 Å-phase is formed from talc + water during quenching. As shown in figure 2B and C, however, the synthesis field of the 10 Å-phase was definitely distinguished from the field where talc existed: the 10 Å-phase was not detected in any runs that had been quenched from temperatures higher than the boundary temperature. This suggests that the 10 Å-phase is not a quench product.

Five phases (brucite, phase D, clinohumite, forsterite, and water) coexist in three runs with different pressure-temperature conditions for x = 70.0 percent shown in table 1 (run 7307 at 29 kb and 815°C, run

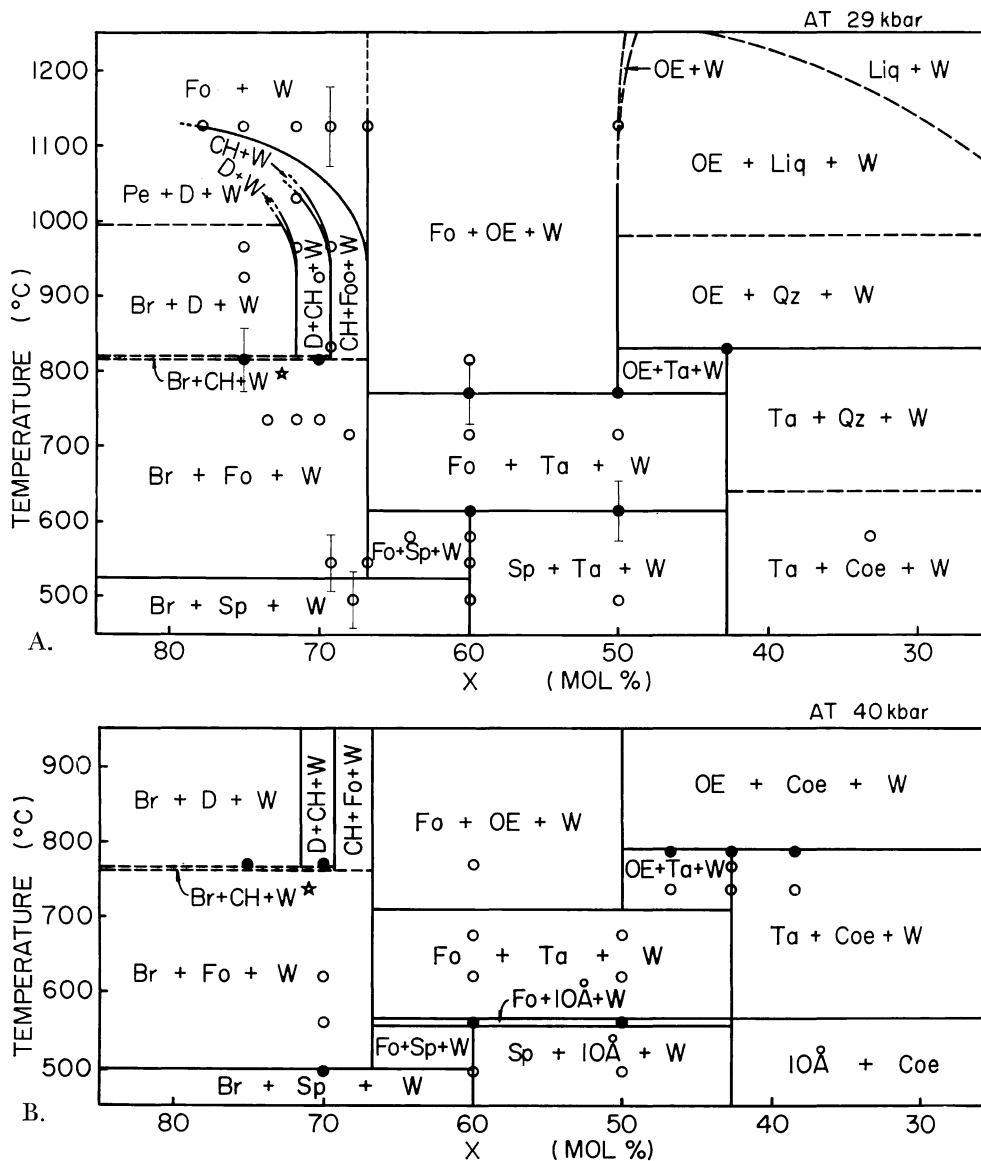
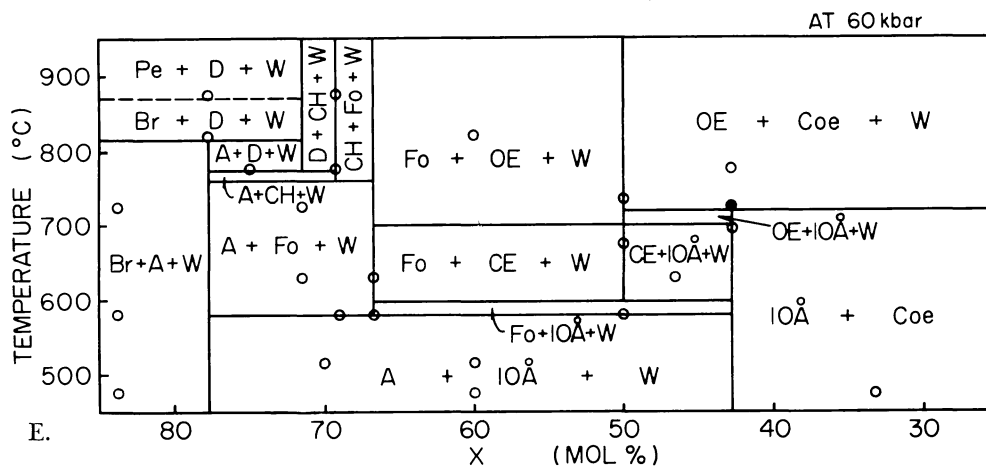
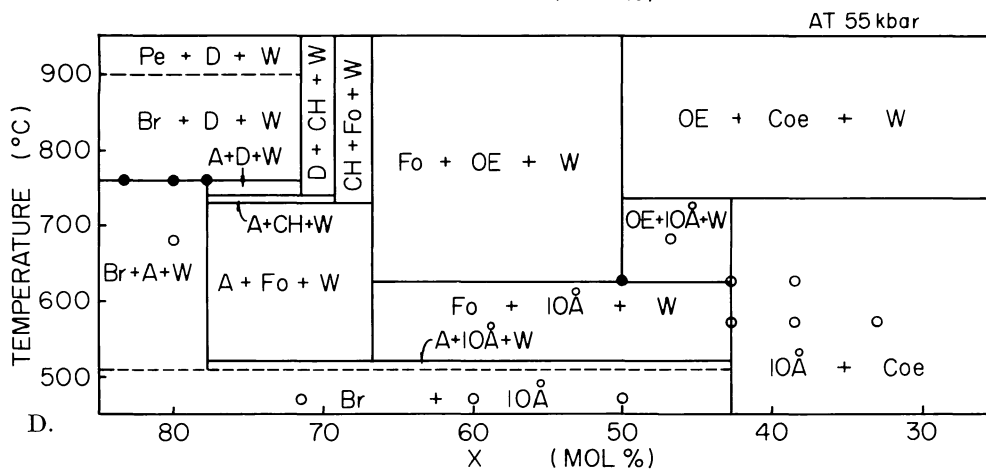
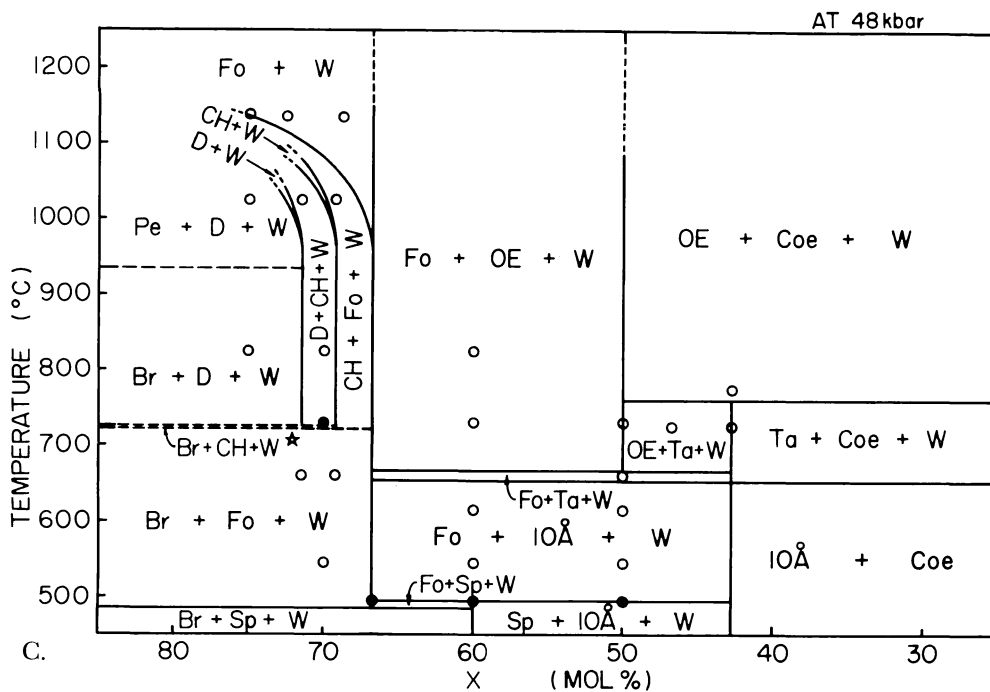


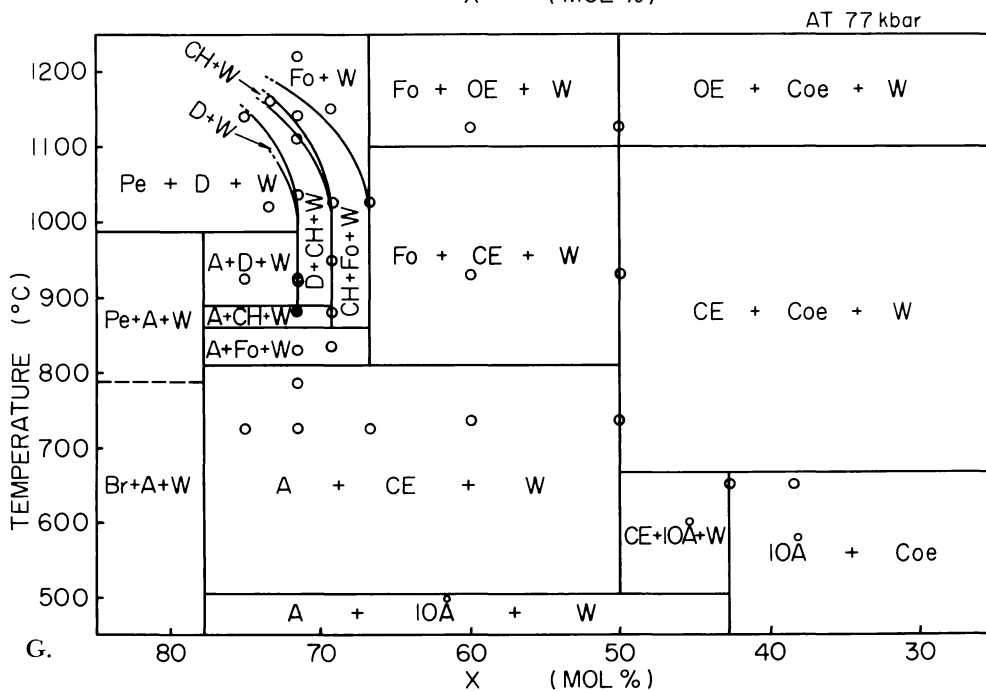
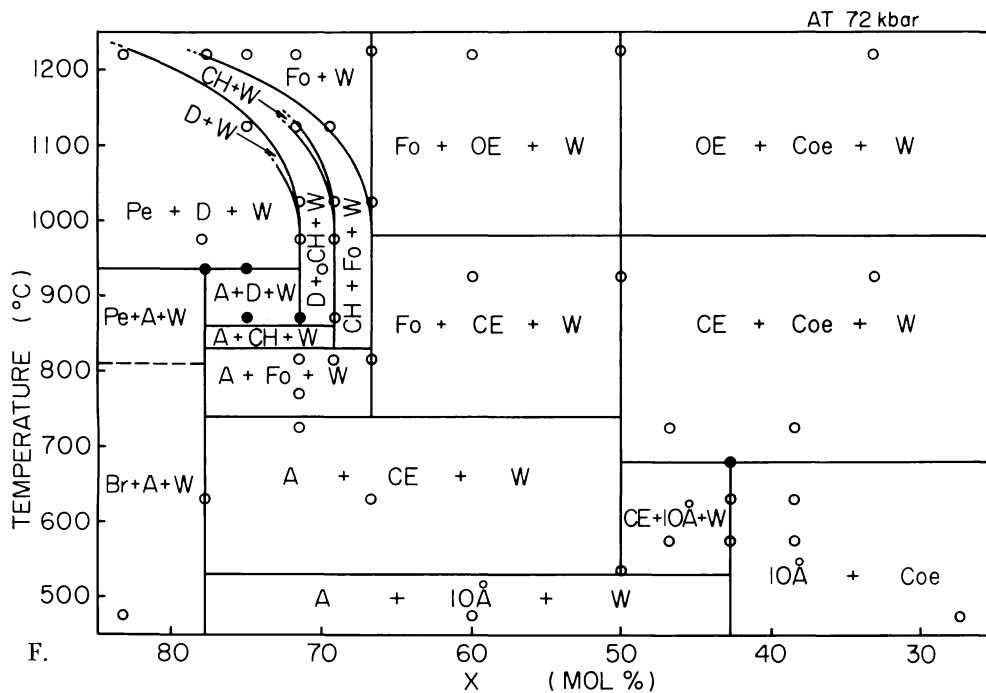
Fig. 2. Isobaric sections of the high pressure and temperature synthesis diagram on the join  $Mg(OH)_2-SiO_2$ : (A) at  $29 \pm 2$  kb; (B) at  $40 \pm 2$  kb; (C) at  $48 \pm 2$  kb; (D) at  $55 \pm 2$  kb; (E) at  $60 \pm 2$  kb; (F) at  $72 \pm 2$  kb; (G) at  $77 \pm 2$  kb.

Experimental runs are represented by open solid circles. The solid circles indicate the runs in which phases on both sides of the boundary line coexisted. Error-bars in (A) represent the maximum uncertainty in temperature measurements:  $\pm 40^\circ C$  at  $600^\circ C$  and  $\pm 50^\circ C$  at  $1000^\circ C$ . The precision of the relative temperature determinations is estimated to be effectively less than  $30^\circ C$ .

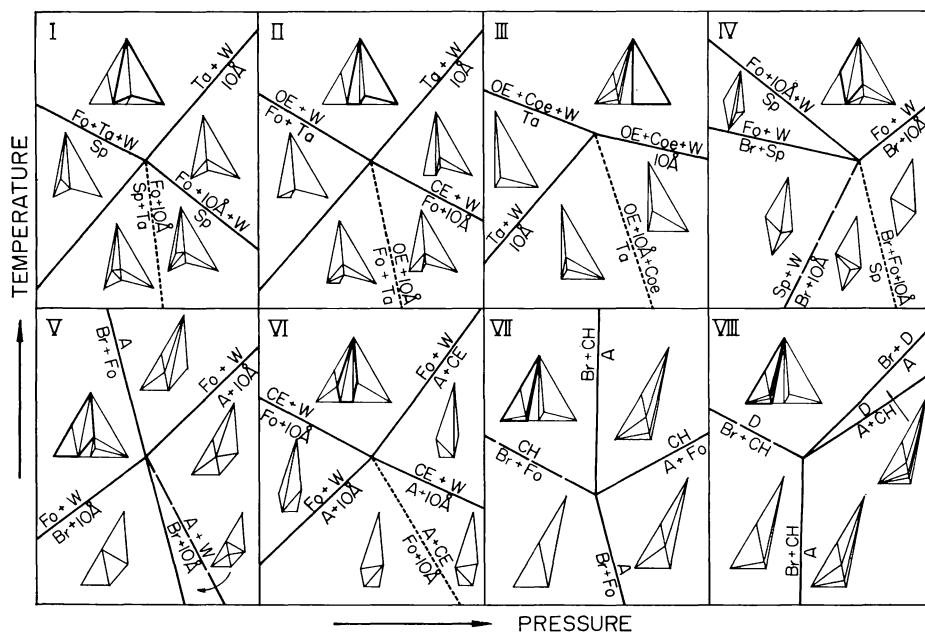
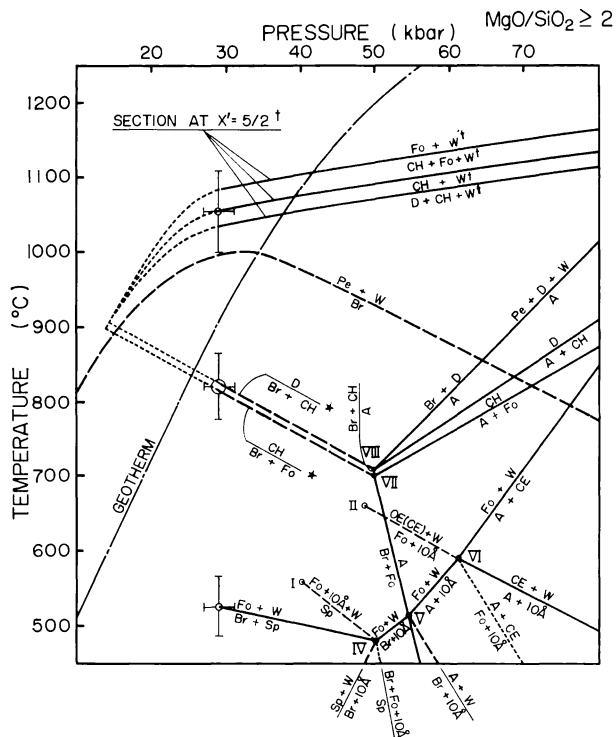
\* Although the field of brucite + clinohumite + water has not been detected, the phase rule requires its presence.

Abbreviations are the same as those in figure 1.









Coexistence of five phases also takes place in two runs for  $x = 50.0$  percent and 60.0 percent at 40 kb and 560°C (run 7319 in table 1). Forsterite, serpentine, talc, 10 Å-phase, and water were observed in these runs. If this pressure-temperature condition were close to an invariant point, the present results are explained. Figures 2B and 3A are constructed based on this interpretation: the narrow field of forsterite + 10 Å-phase + water at the 40 kb-isobar (fig. 2B) is considered to be beyond the resolution of the present temperature measurement and control.

There is still a possibility of the presence of quench products or metastable phases in the runs with five-phases. General views in figure 2A, B, and C, however, are unlikely to develop such a possibility. The runs quenched from temperatures higher than those previously mentioned always produce a reasonable three-phase assemblage. These observations suggest that the quench products are not a problem.

In figures 2 and 3, the equilibrium line between quartz and coesite reported by Boyd (1964) is shown by a broken line. The solidus of quartz and the liquidus of orthoenstatite determined at 20 kb by Kushiro (1969) are shown by a broken line in figure 2A. According to Kushiro, Yoder, and Nishikawa (1968), water coexisting with forsterite and orthoenstatite above 1100°C at 30 kb contains an appreciable amount of silica, and the stability field of forsterite + orthoenstatite + water expands toward the silica-rich region. This is also shown by a broken line in figure 2A.

Results of  $x \geq 66.7$  percent at 72 kb and at temperature above 950°C are shown in figure 4. In the figure, brucite, phase D, clinohumite, and forsterite are expressed by small solid circles, triangles, open circles, and squares, respectively. The stability fields of phase D, clinohumite, and forsterite shift toward a magnesium-rich region with increasing temperatures, with brucite coexisting with these phases when  $x \geq 69.2$  percent. This suggests that the solubility of MgO into H<sub>2</sub>O increases with increasing temperature above 1000°C, therefore the amount of MgO in the solid phase decreases. Chemical potential of MgO in water saturated

TABLE 3  
X-ray diffraction data for Type I of 10 Å-phase

$d_{\text{obs}}$	Intensity	$d_{\text{obs}}$	Intensity
10.24 A	300	2.465 Å B	2
5.116	70	2.399	15
4.784	2	2.159	7
4.764	2	2.046	25
4.512	6	1.987 B	3
4.485	5	1.6774	8
4.343 B	2	1.5450	3
3.638	5	1.5436	3
3.410	100	1.5027 B	2
2.923	7	1.4856	2
2.720	4	1.4843	2
2.593	3	1.4619	3
2.566 B	7	1.3728	10

Abbreviations: B, broad reflection.

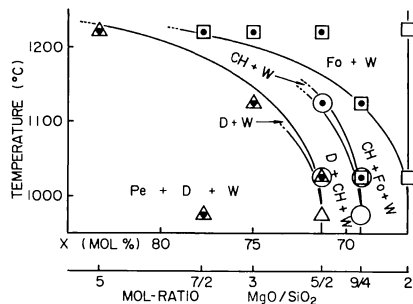


Fig. 4. High-pressure and high-temperature synthesis diagram on the join  $\text{Mg}(\text{OH})_2$ - $(\text{Mg}_2\text{SiO}_4+2\text{H}_2\text{O})$  above  $950^\circ\text{C}$  and 72 kb. Abbreviations: Pe, periclase; D, phase D; CH, clinohumite; Fo, forsterite; W, water; ●, brucite; ▲, phase D; ○, clinohumite; □, forsterite.

with MgO is comparable to that of MgO in phase D and clinohumite and is much larger than that of MgO in forsterite because forsterite is synthesized from mixtures of  $x = 66.7$  percent to  $1225^\circ\text{C}$ . Brucite is formed during quenching of the MgO-bearing fluid. Therefore, four phase assemblages (brucite + phase D + clinohumite + water and brucite + clinohumite + forsterite + water) were frequently obtained in the experiments for  $x \geq 69.2$  percent at temperatures above approx  $1000^\circ\text{C}$ . As shown in table 1 and figure 2A, C, F, and G, this phenomenon was also observed at temperatures above  $965^\circ\text{C}$  and 29 kb, above  $1025^\circ\text{C}$  and 48 kb, above  $1025^\circ\text{C}$  and 72 kb, and above  $1035^\circ\text{C}$  and 77 kb. Pressure dependence on the phenomenon is represented by the phase boundaries in figure 3B, when the system is  $2.666\text{H}_2\text{O} + 2.5\text{MgO} + \text{SiO}_2$  ( $x'=5/2$ ).

X-ray diffraction data of the 10 Å-phase synthesized from  $3\text{Mg}(\text{OH})_2 + 4\text{SiO}_2 + \text{water}$  at  $570^\circ\text{C}$  and 55 kb is given in table 3. It is seen in the table that the  $d$ -spacings of five diffraction lines are approx represented by the equation,

$$d = a/n \quad (1)$$

where  $a = 10.23 \text{ \AA}$  and  $n = 1, 2, 3, 5,$  and  $7$ . The constant  $a$  was determined from the diffraction angle of  $n = 3$  because the angle was close to that of (1 1 1) of silicon which was used as an internal and external standard for the diffraction angles. Since constant  $a$  varies slightly from sample to sample, ranging from 9.81 to 10.23 Å, samples of this phase were classified into two types according to the values of  $a$ : type I with  $a \approx 10.2 \text{ \AA}$ , and type II with  $9.81 \leq a \leq 10.0 \text{ \AA}$ . The type II sample shows diffuse diffraction patterns compared to type I. Samples of type II were not obtained from mixtures of  $x \geq 46.7$  percent. As shown in table 1, both types of samples were synthesized from mixtures of  $x = 38.5$  percent with distilled water under the same condition, 55 kb and  $570^\circ\text{C}$ . The 10 Å-phase was synthesized as a single phase from mixtures of  $x = 42.9$  percent.

Results of the thermal analyses for phase D are summarized in table 4, and the thermogram and differential thermal analysis curve are illus-

trated in figure 5. Figure 5 shows that there are three reaction stages, I, II, and III, in the temperature range from 400° to 1100°C. X-ray diffraction showed no change of the structure during stage I. Just before stage III, a small amount of forsterite and periclase was formed, and a slightly diffuse diffraction pattern of phase D was obtained. After stage III, phase D disappeared, and forsterite and periclase increased in amount. These three reactions are endothermic.

X-ray powder analysis results and measured refractive indices of hydroxyl-clinohumite synthesized in the present experiments are summarized in table 5 together with those of hydroxyl-fluor-clinohumite given in the ASTM card and reported by Deer, Howie, and Zussman (1971). The lattice parameters of hydroxyl-clinohumite were determined as  $a = 13.695 \pm 0.001 \text{ \AA}$ ,  $b = 4.7474 \pm 0.0002 \text{ \AA}$ ,  $c = 10.284 \pm 0.001 \text{ \AA}$ , and  $\beta = 100.64 \pm 0.01^\circ$ . Since the  $d$ -spacings given in the ASTM card are inconsistent with the lattice parameters given in the card, and, furthermore, the indices of the higher order diffraction are not given, the parameters were recalculated as  $a = 13.636 \pm 0.005 \text{ \AA}$ ,  $b = 4.732 \pm 0.001 \text{ \AA}$ ,  $c = 10.228 \pm 0.003 \text{ \AA}$ , and  $\beta = 100.83 \pm 0.03^\circ$ , using the diffraction indices given in table 5. The refractive indices of hydroxyl-clinohumite were measured as  $\alpha = 1.638 \pm 0.002$ ,  $\beta = 1.641 \pm 0.002$ , and  $\gamma = 1.669 \pm 0.001$ . As shown in table 5 the refractive indices of hydroxyl-clinohumite and of hydroxyl-fluor-clinohumite are similar. A Weissenberg camera analysis showed that all seven crystals of clinohumite examined were twinned on the plane (2 0 1), and two were twinned on the plane (1 0 0).

#### DISCUSSION

*Thermal analysis of phase D.*—Since the thermogram and differential thermal analysis curve of phase D shown in figure 5 are similar to those of phase A reported in the previous paper (Yamamoto and Akimoto, 1974), it is reasonable to conclude that the reactions of phase D during the thermal analyses are similar to those of phase A. It is plausible to consider that  $\text{CO}_2$  and  $\text{H}_2\text{O}$  are exhausted during stage I and during stages II and III, respectively.  $\text{MgCO}_3$ , which has been formed by the coupling of some amount of  $\text{Mg}(\text{OH})_2$  in the starting materials with  $\text{CO}_2$  in air before the formation of phase D, still survives in the run

TABLE 4  
Results of thermal analyses for phase D. Synthesized from  
 $5/2 \text{ Mg}(\text{OH})_2 + \text{SiO}_2$  at 50 kb and at about 900°C

Stage	Temperature (°C)	Degree of endotherm	Loss of weight (mg)	Degree of hydration (wt %)
I	410 — 546	a little	0.29	5.3
II	716 — (860)	medium	0.63	
III	(860) — 1063	large	0.52	

Mass of the sample; 21.68 mg

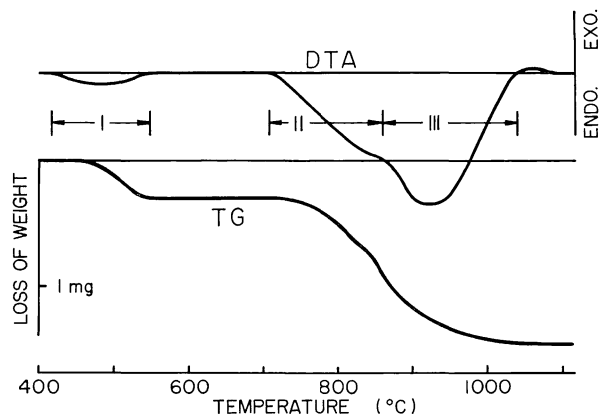


Fig. 5. Thermogram and differential thermal analysis curve for phase D (hydroxyl chondrodite).

products and decomposes in stage I with evolution of  $CO_2$ . Phase D decomposes in stages II and III with evolution of  $H_2O$ . The amount of hydration of phase D was calculated as 5 wt percent from table 3.

*Chemical formula of phase D.*—In the formula for phase D,  $H_LMg_MSi_NO_S$ , L, M, N, and S were determined using the following line of reasoning: Since the refractive indices of phase D are very close to those of hydrated and nonhydrated magnesium silicates, we can assume that the volume per oxygen atom is approx  $18 \text{ \AA}^3$  as in typical magnesium silicates such as forsterite and enstatite. As the volume of a unit cell of phase D is  $368.7 \pm 0.1 \text{ \AA}^3$ , the number of oxygen atoms per unit cell is nominally 20.5. Since phase D belongs to space group  $P2_1/c$ , the number of atoms per unit cell must be even (Norman and Lonsdale, 1969). Consequently, the number of oxygen atoms per unit cell becomes 20, and S is equal to 10. From the chemical formula the following equation must be satisfied.

$$L/2 + M + 2N = S = 10 \quad (2)$$

Phase D + clinohumite were obtained from mixtures of  $x = 70.0$  percent, and brucite + phase D were obtained from mixtures of  $x \cong 73.3$  percent, then

$$0.700 < M/(M+N) < 0.733 \quad (3)$$

Only one set of positive integers,  $L = 2$ ,  $M = 5$ , and  $N = 2$ , satisfies both (2) and (3), so the chemical formula of phase D is determined as  $H_2Mg_5Si_2O_{10}$ ,  $[Mg(OH)_2 \cdot 2Mg_2SiO_4]$ . This conclusion is supported by the amount of hydration calculated from the chemical formula, 5.30 wt percent, which is in good agreement with the measured value.

*Hydroxyl-clinohumite and the structural relation of phase D and hydroxyl-chondrodite.*—The humite group consists of four minerals of which chemical formula are generally expressed by  $Mg(OH,F)_2 \cdot nMg_2SiO_4$  where  $n = 1, 2, 3$ , and 4. The mineral is norbergite where  $n = 1$ ;

TABLE 5  
Data of X-ray diffraction and refractive indices for clinohumite

Mg(OH) <sub>2</sub> ·4Mg <sub>2</sub> SiO <sub>4</sub> (Present work)				Mg(OH,F) <sub>2</sub> ·4Mg <sub>2</sub> SiO <sub>4</sub> (ASTM card)		Mg(OH) <sub>2</sub> ·4Mg <sub>2</sub> SiO <sub>4</sub> (Present work)				Mg(OH,F) <sub>2</sub> ·4Mg <sub>2</sub> SiO <sub>4</sub> (ASTM card)			
h k l	d <sub>obs</sub>	d <sub>calc</sub>	Intensity	d <sub>obs</sub>	Intensity	h k l	d <sub>obs</sub>	d <sub>calc</sub>	Intensity	d <sub>obs</sub>	Intensity		
2 0 0	6.732 Å	6.730 Å	6	5.02 Å	70	3̄ 0 6	1.6825 Å	1.6825 Å	6	1.624 Å	10		
0 0 2	5.049	5.053	50			4.44	30	1 0 6	1.6348			1.6347	15
1̄ 0 2		5.048						4̄ 0 6	1.6321			1.6317	15
3 0 0	4.489	4.487	15	3.86	30	4̄ 2 4	1.6244	1.6244	15	1.612	10		
1 0 2	4.467	4.467	25			6 1 3	1.6223	1.6221	25				
2 0 2	4.456	4.455	25	3.70	70	5̄ 2 4	1.5471	1.5471	10	1.537	10		
1̄ 1 1	4.189	4.190	2			6 0 4	1.5419	1.5421	25				
2 1 0	3.882	3.879	25	3 8 1 3	1.5420	8̄ 0 4		1.5377		1.5375	20		
2 0 2	3.723	3.724	65	3.44	30	2̄ 3 1	1.5324	1.5326	4	1.488	10		
3 0 2	3.714	3.713	60			2 3 1	1.5136	1.5134	6				
2 1 1	3.500	3.499	20	3.35	10	0̄ 0 2	1.5118	1.5121	6	1.479	50		
0 1 2	3.461	3.460	25			0 3 2	1.5100	1.5102	6				
1̄ 1 2		3.458		1̄ 3 2	1.5100	9 0 0		1.4955		1.4955	90		
4 0 0	3.363	3.365	30	3.22	50	3 0 6	1.4891	1.4891	55	1.396	10		
3 1 0	3.262	3.261	8			8̄ 0 6	1.4852	1.4851	60				
1 1 2	3.253	3.253	8	2.91	10	2̄ 1 7	1.4028	1.4029	20	1.345	30		
3 1 1	2.990	2.988	4			4 3 1		1.4026					
3 1 1	3.233	3.233	25	2.76	70	1̄ 1 7	1.3994	1.3995	15				
2 1 2	2.930	2.930	10			3̄ 3 3	1.3967	1.3966	6				
3 1 2	2.926	2.925	12	2.73	50	4 3 2	1.3500	1.3502	20				
1̄ 1 3	2.775	2.775	80			5̄ 3 2	1.3491	1.3492	15				
4 1 1	2.758	2.756	35	2.68	10	1̄ 3 4	1.3474	1.3476	15				
0 1 3	2.748	2.747	40			8 1 3		1.3473					
5 0 0	2.692	2.692	15	2.60	30	1 3 4	1.3219	1.3218	6				
1 1 3	2.616	2.616	35			8̄ 0 6	1.3182	1.3183	4				
5 0 2	2.582	2.582	4	2.54	70	9 1 2	1.3137	1.3136	4				
4 1 2		2.581											
4 1 1	2.553	2.554	65										

$\bar{3}$ 1 3	2.518 Å	2.518 Å	85	2.51 Å	70
2 1 3	2.419	2.419	40	2.40	30
1 0 4	2.404	2.404	25	} 2.39	10
$\bar{3}$ 0 4	2.399	2.399	20		
$\bar{5}$ 1 1	2.366	2.366	60	2.36	50
0 2 1	2.311	2.311	15	2.30	10
4 1 2	2.272	2.273	90	} 2.26	70
$\bar{5}$ 1 2	2.269	2.268	100		
$\bar{1}$ 1 4	2.261	2.261	95		
$\bar{2}$ 2 1	2.215	2.214	8		
5 1 1	2.205	2.205	10	} 2.15	10
3 1 3	2.200	2.200	10		
2 2 1	2.158	2.158	15		
$\bar{3}$ 2 1	2.091	2.091	8		
$\bar{5}$ 1 3	2.086	2.086	8		
$\bar{5}$ 0 4	2.039	2.040	10		
$\bar{1}$ 2 3	1.9501	1.9501	8		
$\bar{1}$ 1 5	1.8860	1.8863	10		
$\bar{6}$ 1 3	1.8816	1.8820	8		
$\bar{2}$ 1 5	1.8765	1.8763	4		
$\bar{6}$ 0 4	1.8560	1.8563	4		
$\bar{3}$ 1 5	1.8315	1.8317	6		
$\bar{7}$ 1 1	1.8087	1.8089	6		
5 2 0	1.7804	1.7804	10		
4 2 2	1.7493	1.7496	90	} 1.742	70
$\bar{5}$ 2 2	1.7474	1.7475	95		
$\bar{1}$ 2 4	1.7446	1.7440	90	1.738	100
$\bar{7}$ 0 4	1.6880	1.6877	15	1.681	10
0 0 6	1.6845	1.6845	10		

Mg(OH) <sub>2</sub> ·4Mg <sub>2</sub> SiO <sub>4</sub> (Present work)	Mg(OH,F) <sub>2</sub> ·4Mg <sub>2</sub> SiO <sub>4</sub> (ASTM card)
Monoclinic (P2 <sub>1</sub> /c)	Monoclinic (P2 <sub>1</sub> /c)
a = 13.695 ± 0.001 Å	a = 13.71 Å
b = 4.7474 ± 0.0002 Å	(13.636 ± 0.005 Å)
c = 10.284 ± 0.001 Å	b = 4.755 Å
β = 100.64 ± 0.01 °	(4.732 ± 0.001 Å)
v = 657.1 ± 0.1 Å <sup>3</sup>	c = 10.29 Å
	(10.228 ± 0.003 Å)
	β = 100.83 °
	(100.83 ± 0.03 °)
	v = 658.7 Å <sup>3</sup>
	(648.1 ± 0.5 Å <sup>3</sup> )
Refractive indices	
(Present work)	(Deer, Hawie and Zussman, 1971)
α = 1.638 ± 0.002	α = 1.629 - 1.638
β = 1.641 ± 0.002	β = 1.641 - 1.643
γ = 1.669 ± 0.001	γ = 1.662 - 1.674

chondrodite where  $n = 2$ ; humite where  $n = 3$ ; and clinohumite where  $n = 4$ . The fluor-humite group compounds were synthesized by Rankama (1947) and Hinz and Kunth (1960). The hydroxyl-fluor-humite group minerals are found in nature and were synthesized by the partial substitution of fluorine of fluorhumite group compounds by OH by Van Valkenburg (1955, 1961). However, no successful synthesis of the hydroxyl-end-members of the humite group has been reported previously in the literature.

As described in the previous paper (Yamamoto and Akimoto, 1974), phase D and chondrodite belong to the same space group  $P2_1/c$ , and their lattice parameters coincide. The chemical formula of phase D and hydroxyl-chondrodite are the same. As shown in table 1 and figures 2, 3B, and 4, the stability field of phase D is similar to that of clinohumite. From these facts one can reasonably conclude that phase D is hydroxyl-chondrodite.

The results of the X-ray analysis of phase D also support the present conclusion. The diffraction intensities of 731 non-equivalent reflections of phase D were measured using an automatic four-circle diffractometer, and the structure refinement was carried out by ordinary techniques using the positional parameters of chondrodite published by Taylor and West (1928) as starting parameters for the full-matrix least-squares program, RSFLS-4 of the program system UNICS (Sakurai, Nakatsu, and Iwasaki, 1967; Fujitsu, 1972) of the Computer Center at Nagoya University. The R-factor,  $(\sum ||F_o| - |F_c|| / \sum |F_o|)$ , reached 0.042, and any maximum or minimum of electron distributions except the maxima considered to be due to protons was not found in the diagrams of the three-dimensional difference synthesis calculated using the program RSSFR-5 in UNICS (Sakurai, 1967). The structure of phase D refined by these measurements was essentially the same as that of natural chondrodite obtained by Gibbs, Ribbe, and Anderson (1970).

The high refractive indices of phase D compared with general chondrodite (Yamamoto and Akimoto, 1974) are probably due to the high polarizability of the hydroxyl ions. Since norbergite and humite were not obtained in the present experiments, it is likely that these phases have no stability field at pressures ranging from 29 to 77 kb. The higher members of the humite group,  $Mg(OH)_2 \cdot nMg_2SiO_4$ , with  $n \geq 5$ , whose existence has been suggested by Bragg and Claringbull (1965), was not synthesized in this study.

*Twinning in clinohumite.*—In the idealized structure of clinohumite (Taylor and West, 1928), oxygen atoms lie in the positions of hexagonal closest packing and magnesium atoms lie parallel to the (2 0 1) plane. The positions of the oxygen atoms have a two-fold rotation symmetry about the axes perpendicular to the (2 0 1) plane. Twinning on the (2 0 1) plane can be formed without introducing a large strain into the lattice. This might be a reason for the frequent observation of this twin in the present experiments. In the idealized structure the positions of oxygen atoms have also a two-fold symmetry about the axes perpen-

dicular to the (1 0 0) plane, and this explains the occurrence of the (1 0 0) twin described in the section on the experimental results.

*Chemical composition of 10 Å-phase.*—The X-ray powder pattern of 10 Å-phase shown in table 2 is similar to the patterns of talc and 3T type of muscovite except the basal spacings. This suggests that the structure of the 10 Å-phase is related to talc as pointed out by Sclar, Carrison, and Schwartz (1965). It is also possible to consider that constant *a* in eq (1) is the basal spacing. From the fact that the observed basal spacings are slightly different from sample to sample, the amount of hydration and the stacking schemes of the successive sheets of linked SiO<sub>4</sub> tetrahedra are probably different in different samples as observed in some kinds of clay minerals. Although Sclar, Carrison, and Schwartz reported that this phase had the composition 5Mg(OH)<sub>2</sub> • 8SiO<sub>2</sub>, the present experimental results indicate that the composition is close to 3Mg(OH)<sub>2</sub> • 4SiO<sub>2</sub>. Unfortunately, since crystals of 10 Å-phase are too small to be examined by the Weissenberg camera, the crystal structure and the exact chemical formula could not be determined. Therefore, the formula 3Mg(OH)<sub>2</sub> • 4SiO<sub>2</sub> of 10 Å-phase is used as an approximation in figures 1 and 2.

*Comparison with previous studies.*—Kitahara, Takenouchi, and Kennedy (1966) determined the equilibrium curves of the following reactions below 30 kb,

- (i) talc  $\rightleftharpoons$  orthoenstatite + quartz + water
- (ii) talc + forsterite  $\rightleftharpoons$  orthoenstatite + water
- (iii) serpentine  $\rightleftharpoons$  forsterite + talc + water
- (iv) brucite + serpentine  $\rightleftharpoons$  forsterite + water

These curves are shown by dotted lines in figure 3A. Our results for reactions (i), (iii), and (iv) agree within experimental errors at 30 kb. Present results for reaction (ii), however, are approx 80°C higher. Although this difference is within the limit of the maximum uncertainty due to the experimental errors for pressure and temperature determinations, there is a possibility of disequilibrium in the fairly short critical runs in this study. The exact position and curvature of curve (ii) must be determined by reversed reaction experiments using a high pressure and temperature apparatus which is suitable for long runs. Kitahara, Takenouchi, and Kennedy constructed a phase diagram of the system MgO-SiO<sub>2</sub>-H<sub>2</sub>O at 30 kb, which is almost identical with figure 2A except for the absence of phase D and clinohumite.

The equilibrium curves of the transition, orthoenstatite  $\rightleftharpoons$  clinoenstatite determined by Sclar, Carrison, and Schwartz (1964), Boyd and England (1965), and Grover (1972), are shown by dotted lines in figure 3A. Present results are significantly different from these previous determinations. According to Riecker and Rooney (1967), Coe (1970), and Smyth (1974), the transition is affected by shear stress. Although shear stress is probably not significant when water is present as a phase in these experiments, it may be significant at the initial stage during the period

of the nucleation and at the time of quenching when the high-pressure polymorphs of ice are formed. Therefore, the phase boundary between orthoenstatite and clinoenstatite shown in figures 2 and 3 represents only the boundary of the synthesis fields of these phases.

*Geological application.*—It is found in figure 3A and B that the 10 Å-phase can coexist with both forsterite and enstatite at relatively low temperature and high pressure condition: its upper stability limit is approx 650°C at 48 kb. This suggests that the 10 Å-phase could be stable only in the subduction zone in the upper mantle. Phase A can coexist with forsterite and enstatite up to 800°C at 77 kb and could also be stable in the subduction zone.

As seen in figure 3B, clinohumite and chondrodite are stable for nearly the same pressure-temperature conditions, ranging between approx 700° and 1100°C and 29 to 77 kb. It is noted that they are stable even along the continental geotherm (Herrin, 1972) at depths between 70 and 120 km. Although both clinohumite and chondrodite are stable only in rocks much richer in MgO than the accepted mantle rocks, they are of considerable interest as possible sites for H<sub>2</sub>O in the upper mantle. The present experiments also confirm the petrological inference by McGetchin, Silver, and Chodos (1970) that titanoclinohumite in the Moses Rock kimberlite,  $x[\text{TiO}_2 \cdot 4\text{Mg}_2\text{SiO}_4] \cdot (1-x)[\text{Mg}(\text{OH},\text{F})_2 \cdot 4\text{Mg}_2\text{SiO}_4]$ , where  $1 > x > 0$  had equilibrated in the mantle at depth ranging from approx 50 to 150 km at moderately high temperatures generally less than 1000°C before transport to the surface during the emplacement of the kimberlite.

Nakamura and Kushiro (1974) suggested on the basis of their experiments on the Mg<sub>2</sub>SiO<sub>4</sub>-SiO<sub>2</sub>-H<sub>2</sub>O system that water passing upward through the upper mantle peridotite will carry large amounts of SiO<sub>2</sub> in solution, leaving the mantle as a whole relatively depleted in SiO<sub>2</sub>. As Ringwood (1975, 1976) suggested, this effect substantially increases the pressure-temperature stability fields of clinohumite and chondrodite in the upper mantle. Since there is little doubt that appreciable amounts of water are present in the subducting lithosphere, it is likely that both clinohumite and chondrodite are also the possible H<sub>2</sub>O-bearing mineral phases in the subduction zone and the overlying peridotite wedge.

#### ACKNOWLEDGMENTS

The authors thank Drs. G. Hashizume and K. Amita of the Industrial Research Institute, Hyogo Prefecture, for their helpful comments and permission to use the instrument of the thermal analyses. The authors are greatly indebted to Drs. K. Suwa and Y. Tsuzuki of Nagoya University for their useful comments on the optical study. The X-ray diffraction intensity data of phase D were collected with the help of Prof. J. Tanaka and Dr. C. Katayama of Nagoya University. Their kind permission to use the automatic four-circle diffractometer is gratefully acknowledged. The authors are heartily grateful to Dr. Y. Nakamura of University of Tokyo whose critical review was very helpful for the improvement of the present paper.

REFERENCES

- Akimoto, S., Fujisawa, H., and Katsura, T., 1965, The olivine-spinel transition in  $Fe_2SiO_4$  and  $Ni_2SiO_4$ : *Jour. Geophys. Research*, v 70, p. 1969-1977.
- Bowen, N. L., and Tuttle, O. F., 1949, The system  $MgO-SiO_2-H_2O$ : *Geol. Soc. America Bull.*, v. 60, p. 439-460.
- Boyd, F. R., 1964, Geological aspects of high-pressure research: *Science*, v. 145, p. 13-20.
- Boyd, F. R., and England, J. L., 1965, The rhombic enstatite-clinoenstatite inversion: *Carnegie Inst. Washington Year Book* 64, p. 117-120.
- Bragg, L., and Claringbull, G. F., 1965, *Crystal structures of minerals*: London, G. Bell and Sons, 409 p.
- Coe, R. S., 1970, The thermodynamic effect of shear stress on the ortho-clino inversion in enstatite and other coherent phase transitions characterized by a finite simple shear: *Contr. Mineralogy Petrology*, v. 26, p. 247-264.
- Deer, W. A., Howie, R. A., and Zussman, J., 1971, *An introduction to the rock forming minerals*: London, Longmans, 528 p.
- Fujitsu, 1972, FACOM 230-60 UNICS (in Japanese): Tokyo, Fujitsu, no. 60505013-1, 255 p.
- Gibbs, G. V., Ribbe, P. H., and Anderson, C. P., 1970, The crystal structures of the humite minerals: II. chondrodite: *Am. Mineralogist*, v. 55, p. 1182-1194.
- Grover, J., 1972, The stability of low-clinoenstatite in the system  $Mg_2Si_2O_6-CaMgSi_2O_6$  [abs.]: *Am. Geophys. Union Trans.*, v. 53, p. 539.
- Herrin, E., 1972, A comparative study of upper mantle models: Canadian shield and basin and range provinces, in Robertson, E. C., Hays, J. F., and Knopoff, L., eds., *The nature of the solid earth*: New York, McGraw Hill, p. 216-231.
- Hinz, W., and Kunth, P. O., 1960, Phase equilibrium data for the system  $MgO-MgF_2-SiO_2$ : *Am. Mineralogist*, v. 45, p. 1198-1210.
- Kitahara, S., Takenouchi, S., and Kennedy, G. C., 1966, Phase relations in the system  $MgO-SiO_2-H_2O$  at high temperatures and pressures: *Am. Jour. Sci.*, v. 264, p. 223-233.
- Kushiro, I., 1969, The system forsterite-diopside-silica with and without water at high pressures: *Am. Jour. Sci.*, v. 267-A. Schairer v., p. 269-294.
- Kushiro, I., Yoder, H. S., and Nishikawa, M., 1968, Effect of water on the melting of enstatite: *Geol. Soc. America Bull.*, v. 79, p. 1685-1692.
- McGetchin, T. R., Silver, L. T., and Chodos, A. A., 1970, Titanite-clinohumite: a possible mineralogical site for water in upper mantle: *Jour. Geophys. Research*, v. 75, p. 255-259.
- Nakamura, Y., and Kushiro, I., 1974, Composition of the gas phase in  $Mg_2SiO_4-SiO_2-H_2O$  at 15 kbar: *Carnegie Inst. Washington Yearbook* 73, p. 255-258.
- Norman, F. M. H., and Lonsdale, K., 1969, *International tables for X-ray crystallography*, v. I, Symmetry groups: Birmingham, England, Kynock Press, 558 p.
- Rankama, K., 1947, Synthesis of norbergite and chondrodite by direct dry fusion: *Am. Mineralogist*, v. 32, p. 146-157.
- Riecker, R. E., and Rooney, T. P., 1967, Deformation and polymorphism of enstatite under shear stress: *Geol. Soc. America Bull.*, v. 78, p. 1045-1054.
- Ringwood, A. E., 1975, *Composition and Petrology of the Earth's mantle*: New York, McGraw-Hill, 618 p.
- 1976, Phase transformations in descending plates and implications for mantle dynamics: *Tectonophysics*, v. 32, p. 129-143.
- Ringwood, A. E., and Major, A., 1967, High pressure reconnaissance investigations in the system  $Mg_2SiO_4-MgO-H_2O$ : *Earth Planetary Sci. Letters*, v. 2, p. 130-133.
- Sakurai, T., 1967, RSSFR-5, general Fourier synthesis (and structure factor), in Sakurai, T., ed., *Universal Cryst. Computation Program System (UNICS) I.* (in Japanese): Tokyo, Cryst. Soc. Japan, p. 45-52.
- Sakurai, T., Nakatsu, K., and Iwasaki, J., 1967, RSFLS-4, Full-matrix structure factor, least-squares, in Sakurai, T., ed., *Universal Cryst. Computation Program System (UNICS) I.* (in Japanese): Tokyo, Cryst. Soc. Japan, p. 61-65.

- Sclar, C. B., and Carrison, L., 1966, High-pressure reactions and shear strength of serpentized dunite: *Science*, v. 153, p. 1285-1286.
- Sclar, C. B., Carrison, L. C., and Schwartz, C. M., 1964, High-pressure stability field of clinoenstatite and the orthoenstatite-clinoenstatite transition [abs.]: *Am. Geophys. Union Trans.*, v. 45, p. 121.
- 1965, High-pressure synthesis and stability of a new hydronium-bearing layer silicate in the system MgO-SiO<sub>2</sub>-H<sub>2</sub>O [abs.]: *Am. Geophys. Union Trans.*, v. 46, p. 184.
- Smyth, J. R., 1974, Experimental study on the polymorphism of enstatite: *Am. Mineralogist*, v. 59, p. 345-352.
- Taylor, W. H., and West, J., 1928, The crystal structure of the chondrodite series: *Royal Soc. London Proc.*, A-117, p. 517-532.
- Van Valkenburg, A., 1955, Synthesis of the humites: *Am. Mineralogist*, v. 40, p. 339.
- 1961, Synthesis of the humites nMg<sub>2</sub>SiO<sub>4</sub> • Mg(F,OH)<sub>2</sub>: *Natl. Bur. Std. Jour. Research*, A-65, p. 415-428.
- Yamamoto, K., and Akimoto, S., 1974, High pressure and high temperature investigations in the system MgO-SiO<sub>2</sub>-H<sub>2</sub>O: *Solid State Chemistry Jour.*, v. 9, p. 187-195.
- Yamaoka, S., Fukunaga, O., and Saito, S., 1970, Phase equilibrium in the system MgO-H<sub>2</sub>O at high temperatures and very high pressures: *Am. Ceramic Soc. Jour.*, v. 53, p. 179-181.